Physica B: Condensed Matter 547 (2018) 1–5

Contents lists available at ScienceDirect

Physica B: Condensed Matter

journal homepage: www.elsevier.com/locate/physb

Strain effect on the electronic properties of Ce-doped SnS_2 monolayer

Guizhen Qiu[a], Huimin Zhang[a], Yaming Liu[b,*], Congxin Xia[c,**]

[a] Xinxiang Medical University, Xinxiang, 453003, China
[b] Henan Institute of Science and Technology, Xinxiang 453003, China
[c] Henan Normal University, Xinxiang 453003, China

ARTICLE INFO

Keywords:
First-principles
Ce-doped SnS_2 monolayer
Effect of strain
Electronic property

ABSTRACT

First-principles calculations based on density functional theory are carried out to investigate the formation energy, transition energy level, electronic structure and effect of strain on Ce-doped SnS_2 monolayer nanosheet. Numerical results show that the doped nanocompound is energetically stable, while the introduced dopant state is composed completely of *Ce_4f* electrons, and the adopted perfect SnS_2 monolayer leads to the disagreement with experimental Ce^{3+} ionic state. Applying biaxial strain from −10% to +10%, the doped system holds the indirect semiconducting characteristics in the strain range −4%~+6%. The variation tendency of bandgaps is almost to be a horizontal line about 1.9eV under compressive conditions, and the bandgaps increase slowly at first and then decrease rapidly beyond +4%. This work is useful for further improving Ce-doped SnS_2 nanostructures and paves the way in the potential application in photocatalysis and lithium-ion battery.

1. Introduction

Due to the peculiar geometrical structure, abundant reserves, excellent chemical stability in acid conditions, nontoxicity and environmental friendliness, the layered two-dimensional (2D) semiconductor SnS_2, has been receiving intensive attention for the applications in next-generation nanoelectronics, optoelectronics, photocatalysis and lithium-ion battery [1–9]. A series of experiments show that doping with Cu, Zn, In, Ag, etc, the composites exhibit enhanced visible light-driven photocatalytic activity, and can be candidates for environmental remediation and energy conversion [10–15]. Doping with V, W, Fe, etc, the bandgaps are engineered, and the systems can be used as solar energy absorbers in photovoltaic devices [16–20]. Recent experiments show that Ce-doped SnS_2 nanocomposites exhibit both higher photocatalytic activity and significantly improved electrode cycling performance and rate retention ability in lithium-ion batteries [21,22]. Except for these metal dopants, controlling the Se composition in $SnSe_xS_{2-x}$ ternary alloys, the carrier mobility of the 2D nanosheets can be effectively tuned and showing excellent optoelectronic properties [23,24]. To address the characterization of the nature of these dopants, theoretical works are highly in demand, and tremendous reports are carried out to explore the mechanism and underlying reasons [25–35].

To the best of our knowledge, however, theoretical investigations related to the Ce-doped SnS_2 systems have not been reported yet. The doped geometrical structures, variation of electrical properties, effect of strain as well as the mixing behavior, are still unclear from a theoretical point of view. In this work, we focus on the Ce-doped SnS_2 monolayer, and the mentioned issues will be systematically calculated under density functional theory (DFT) framework.

2. Computational methods

All the first-principles calculations in this work are carried out using VASP [36,37]. The Perdew-Burke-Ernzerhof (PBE) parameterization of the generalized-gradient approximation (GGA) is employed to model the exchange and correlation interactions [38,39]. Projected augmented-wave (PAW) method is adopted to describe the electron-ion potential [40]. A kinetic energy cutoff of 520eV is selected for the plane wave expansion, and the Γ-centered Monkhost-Pack *k*-points grid of $5 \times 5 \times 1$ and $11 \times 11 \times 1$ are choosed in the atomic and electronic calculations [41]. The geometrical structure of the crystal is determined by optimizing the atomic positions using CG method with a force convergence criterion of 10^{-3} Å to precisely harvest the energy bandgaps, the valence electron configurations considered here are S ($3s^23p^4$), Sn ($4d^{10}5s^25p^2$) and Ce ($5s^25p^66s^24f^15d^1$). The effect of on-site coulomb repulsion of *Sn_4d* and *Ce_4f* states is treated by GGA + U approach [42], and the *U* values are choosed respectively as 9.0eV and 6.3eV for *Sn_4d* and *Ce_4f*. These values are successfully used in several

* Corresponding author. Henan Institute of Science and Technology, Xinxiang 453003, China.
** Corresponding author. Henan Normal University, Xinxiang 453003, China.
E-mail addresses: liuym@hist.edu.cn (Y. Liu), xiacongxin@htu.cn (C. Xia).

https://doi.org/10.1016/j.physb.2018.07.032
Received 6 June 2018; Received in revised form 15 July 2018; Accepted 30 July 2018
Available online 01 August 2018
0921-4526/

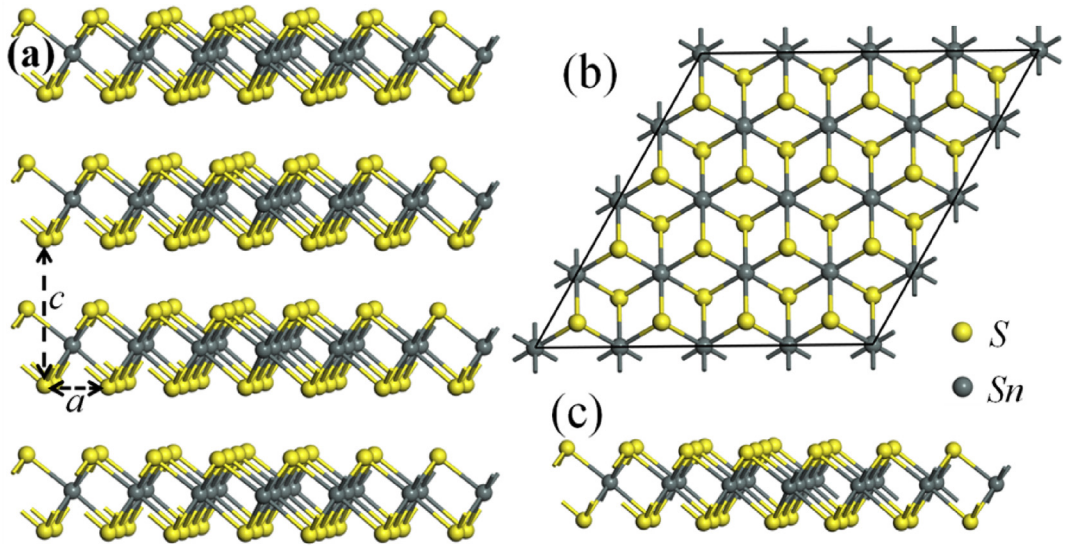

Fig. 1. Schematics of SnS_2 in different structures. (a) 2H-type (P-3m1), lattice parameters *a* and *c* are marked in dashed arrows(b) top and (c) side view of 4 × 4 supercell of monolayer SnS_2.

present theoretical works [28,43]. To describe the non-bonding weak van der Waals interactions between the layers of bulk SnS_2, the Grimme's DFT-D2 method is considered [44].

3. Results and discussions

3.1. Structures of bulk and monolayer SnS_2

Bulk SnS_2 is an *n*-type layered semiconductor, each layer has an S−Sn−S sandwich-like structure, and the layers are weakly coupled by van der Waals interactions. Periodically stacking along *c*-direction, the triple-layers result in many different polytypes. The simplest and most common polytype belongs to space group *P-3m1* (No.164), and denoted as 2H− SnS_2, (H-for hexagonal) see Fig. 1. Here, we choose the 2H− SnS_2 as the parent bulk crystal phase. Independent of the different bulk phase, the exfoliated monolayer SnS_2 nanosheet adopts only the space group P-3m1. To simulate the monolayer, a supercell consisting of 4 × 4 formula units with 16 Sn atoms and 32 S atoms (*i.e.* $Sn_{16}S_{32}$) is constructed.

The optimized geometrical and electronic structures of bulk and monolayer SnS_2 are listed in Table 1, and compared with previous experimental and theoretical data.

Due to the well-known shortcoming of DFT, the PBE functional overestimates the in-plane lattice constant *a* of the bulk phase by 1.4%, whereas the error of out-of-plane lattice parameter *c* is approximately 14.8%. Applying the Grimme's DFT + D2 method to the bulk phase, a proper description with error of *c* are less than 4% is obtained. As for the monolayer SnS_2, PBE functional results in better lattice constant than that of PBE + *U* approach. However, compared with the reported experimental data, the effect of on-site Hubbard *U* can lead to excellent bandgaps. To harvest moderate electronic properties, the PBE + *U* method will be applied to all the following calculations.

Table 1
Lattice constants, S−Sn bond lengths $d_{S\text{-}Sn}$ and band gaps E_g of SnS_2 in different crystal structures calculated with different DFT frameworks, and compared with previous theoretical and experimental reports.

	Bulk (2H-phase)		monolayer	
	D2 + *U* (+*U*)	Reference	PBE(+*U*)	Reference
a(Å)	3.573 (3.701)	3.649 [1]	3.689 (3.482)	3.700 [3]
c(Å)	6.159 (6.774)	5.899 [1]	–	–
$d_{S\text{-}Sn}$(Å)	2.485 (2.596)	2.467 [28]	2.591 (2.437)	2.600 [3]
E_g (eV)	2.141 (1.660)	1.926 [28]	1.650 (2.362)	2.230 [3]

Fig. 1(c) shows the electronic band structures of monolayer and bulk 2H− SnS_2. We find that the valence band maximum (VBM) of both panels locate along Γ–M high symmetry line and near the Γ-point. While the conduction band minimum (CBM) lies respectively at M and L point for monolayer and 2H− SnS_2, indicating the indirect semiconducting characteristic. Due to the reduction of dimensionality from 3D-bulk to 2D-monolayer structure, the M point of monolayer is equivalent to L-point of bulk phase in the Brillouin zone [20]. The calculated bandgaps agree well with the present experimental reports. Rechecking the band structures of 2H− SnS_2, the energy curves along the Γ–K–M–Γ are similar to that along A–H–L–A, which implies that the interaction along c-axis is weak, and coincides with the characteristic of layered van der Waals compounds.

3.2. Structure and stability of Ce-doped monolayer SnS_2

Recent experiments found that Ce-doped SnS_2 nanostructures exhibit higher photocatalytic activity and better performance in lithium-ion battery. To have a microscopic scenario and better understanding of the substitutional behavior, the formation energy (E_{form}), transition energy level, geometrical structure and electronic properties of Ce-doped monolayer SnS_2 is systematically discussed. Though the following equation

$$E_{form}(Ce^q) = E[Ce^q] - E[SnS_2] + \mu_{Ce} + q[E_F + E_V + \Delta V],$$

the formation energy is calculated, where E [Ce^q] and E [SnS_2] are the calculated total energies of Ce-doped and pristine monolayer SnS_2 with the same size. E_F is the Fermi level referenced to the energy position (EV) of the valence band maximum (VBM) of pristine monolayer SnS_2. The correction term ΔV is used to align the reference potential of the doped compounds to that of the pristine supercell. μ_X is chemical potential of corresponding X (X = Sn, S, Ce) and the magnitudes of μ_X depend on growth conditions. In X-rich environments, μ_X is the total energy per atom in its reference phase. Here, we adopt the most energetic stable cubic phase for Ce (No.225) and Sn (No.227), while S2 molecular is used for sulfur atom. To maintain a stable SnS_2 nanosheet, μ_X of S and Sn must satisfy $\mu_{Sn} + 2\mu_S = \mu_{SnS2}$. μ_{SnS2} is the total energy of one formula in nanosheet reference phase. Thus, the formation energies of the Ce-doped compounds are 1.249eV and −3.201eV for Sn-rich and S-rich growth conditions. The negative E_{form} under S-rich condition